Water Research 200 (2021) 117271

Contents lists available at ScienceDirect

Water Research

journal homepage: www.elsevier.com/locate/watres

Effect of granular activated carbon and other porous materials on thermal decomposition of per- and polyfluoroalkyl substances: Mechanisms and implications for water purification

Pavankumar Challa Sasi[a], Ali Alinezhad[a], Bin Yao[a,b], Alena Kubátová[b], Svetlana A. Golovko[c], Mikhail Y. Golovko[c], Feng Xiao[a,*]

[a] Department of Civil Engineering, University of North Dakota, 243 Centennial Drive Stop 8115, Grand Forks, North Dakota 58202, United States
[b] Department of Chemistry, University of North Dakota, 151 Cornell Street Stop 9024, Grand Forks, North Dakota 58202, United States
[c] Department of Biomedical Sciences, University of North Dakota, 1301 Columbia Road North Stop 9037, Grand Forks, North Dakota 58202, United States

ARTICLE INFO

Article history:
Received 29 December 2020
Revised 8 May 2021
Accepted 15 May 2021
Available online 19 May 2021

Keywords:
GAC regeneration
Thermal degradation
Long-chain PFAS
Short-chain PFAS
HFPO-DA
High-resolution mass spectrometry

ABSTRACT

Thermal treatment is routinely used to reactivate the spent granular activated carbon (GAC) from water purification facilities. It is also an integral part of sewage sludge treatment and municipal solid waste management. This study presents a detailed investigation of the fate of per- and polyfluoroalkyl substances (PFAS) and one PFAS alternative (GenX) in thermal processes, focusing on the effect of GAC. We demonstrate that the thermolysis of perfluoroalkyl carboxylic acids (PFCAs), including perfluorooctanoic acid (PFOA), and GenX can occur at temperatures of 150–200 °C. Three temperature zones were discovered for PFOA, including a stable and nonvolatile zone (≤90 °C), a phase-transfer and thermal decomposition zone (90–400 °C), and a fast decomposition zone (≥400 °C). The thermal decomposition began with the homolysis of a C–C bond next to the carboxyl group of PFCAs, which formed unstable perfluoroalkyl radicals. Dual decomposition pathways seem to exist. The addition of a highly porous adsorbent, such as GAC or a copolymer resin, compressed the intermediate sublimation zone of PFCAs, changed their thermal decomposition pathways, and increased the decomposition rate constant by up to 150-fold at 250 °C. The results indicate that the observed thermal decomposition acceleration was linked to the adsorption of gas-phase PFCA molecules on GAC. The presence of non-activated charcoals/biochars with a low affinity for PFOA did not accelerate its thermal decomposition, suggesting that the π electron-rich, polyaromatic surface of charcoal/GAC played an insignificant role compared to the adsorbent's porosity. Overall, the results indicate that (1) substantial decomposition of PFCAs and GenX during conventional thermal GAC/sludge/waste treatment is very likely, and (2) the presence or addition of GAC or other highly porous materials can accelerate thermal PFAS decomposition and alter decomposition pathways.

1. Introduction

Per- and polyfluoroalkyl substances (PFAS) are anthropogenic chemicals that have been produced for decades as either processing aids or individual ingredients in many industrial and commercial products, including aqueous film-forming foams (Barzen-Hanson et al., 2017; Houtz et al., 2013), non-stick cookware (Begley et al., 2005; Sajid and Ilyas, 2017), and fast-food packaging (Schaefer et al., 2017). Perfluoroalkyl substances comprise compounds such as perfluorooctanoic acid (PFOA) and perfluorooctanesulfonic acid (PFOS) in which C–F bonds have replaced C–H bonds in nonfluorinated counterparts. Perfluoroalkyl substances are chemically and biologically recalcitrant (Schröder and Meesters, 2005; Sinclair and Kannan, 2006; Xiao et al., 2012), whereas polyfluoroalkyl substances, including cationic or zwitterionic PFAS, are subject to degradation (Houtz et al., 2016; Jin et al., 2020; Lee et al., 2010; Nabb et al., 2007; Xiao et al., 2018). Once released to the natural environment, long-chain PFAS (≥7 perfluorocarbons) can bioaccumulate and biomagnify through food webs (Houtz et al., 2016; Jin et al., 2020; Langberg et al., 2019; Xiao et al., 2013a). PFOA and PFOS have been reported in >95% of blood samples collected during multiple U.S. national surveys (NHANES, 2014) at concentrations that are a risk to human health (DeWitt et al., 2018; Grandjean et al., 2012; Melzer et al., 2010; Steenland et al., 2010). PFAS-contaminated drinking water is an important source of exposure for the general population

* Corresponding author.
E-mail addresses: fxiaoee@gmail.com, Feng.Xiao@UND.edu (F. Xiao).

https://doi.org/10.1016/j.watres.2021.117271
0043-1354/

(Boiteux et al., 2012; Ericson et al., 2009; Hoffman et al., 2011; Post et al., 2012; Vestergren and Cousins, 2009). PFAS are recalcitrant to degradation at ambient temperature and atmospheric pressure, and are not easily removed in conventional drinking-water and wastewater treatment processes (Anumol et al., 2016; Appleman et al., 2014; Eschauzier et al., 2012; Liu et al., 2020; Rahman et al., 2014; Xiao et al., 2012; Xiao et al., 2013b; Yu et al., 2009a). In fact, Xiao et al. demonstrated that PFOA and PFOS are generated from certain cationic/zwitterionic polyfluoroalkyl compounds during water disinfection by chlorine or ozone (Xiao et al., 2018). The U.S. EPA recently set a drinking water advisory on the combined level of PFOA and PFOS at 0.070 μg/L, making the removal of these compounds from drinking water a health priority.

Adsorption by granular activated carbon (GAC) is frequently used to remove PFAS from drinking water at full-scale treatment operations (Belkouteb et al., 2020; ; Rahman et al., 2014; Yu et al., 2009b). The spent or exhausted GAC can be reactivated or regenerated, used as a fuel for combustion, or deposited in a landfill, depending on whether or not it is nonhazardous (Council, 2009). Information on the fate of PFAS during GAC thermal treatments (regeneration or combustion) is meager. Watanabe et al. studied the decomposition of PFOA, perfluoroheptanoic acid (PFHpA), and PFOS on GAC at 700 °C (Watanabe et al., 2018). The authors observed a 99% decomposition efficiency of these chemicals at 700 °C (Watanabe et al., 2018). The decomposition rates at other temperatures were not determined (Watanabe et al., 2018). Gerhard and co-workers found that the thermal treatment of PFAS-loaded GAC at high temperatures (1011–1048 °C) resulted in near complete degradation of PFAS (e.g., >99.8%) (Duchesne et al., 2020). Xiao et al. investigated the thermal stability and decomposition of several short- and long-chain PFAS on GAC within a wide temperature range of 25–900 °C (Xiao et al., 2020). The authors also developed a method for PFAS extraction from GAC (Xiao et al., 2020). The term 'thermal stable' has been frequently used to describe PFAS in the literature. However, Xiao et al. observed 94.95–99.99% decomposition of perfluoroalkyl carboxylic acids (PFCAs) on GAC after a 30-min thermal treatment at low temperatures (200–300 °C) (Xiao et al., 2020). The authors also found that the degradation of PFAS in GAC varied insignificantly between different atmospheric environments (N_2, CO_2, O_2) (Xiao et al., 2020). This discovery raises the question on the nature of PFAS thermal decomposition. Can perfluoroalkyl substances be thermally degraded at 200 °C without the presence of GAC? If so, how fast is this process? Does GAC facilitate the thermal degradation of these compounds? If yes, what is the relative importance of the polyaromatic surface and the porosity of GAC? Answering these questions has important implications for understanding the fate of PFAS in thermal water/wastewater/sludge/waste treatment processes.

Two important structural features of porous pyrogenic carbonaceous materials (PCMs), including GAC, are the porosity and polyaromatic units (Kah et al., 2017). An analogy can be drawn between polyaromatic units of porous PCMs and the hexagonal sp^2-carbon ("graphene") sheets that make up the surface of graphite, graphene materials, and carbon nanotubes. The polyaromatic units jumble disorderedly to create nanopore networks. During the activation step of GAC production, oxidative gases enter these networks, remove obstructions such as tarry materials, and open more pore networks.

The PCM family also includes natural charcoals generated during the incomplete combustion, or pyrolysis, of lignocellulosic biomass (Glover et al., 2018; Lehmann and Joseph, 2009; Schmidt and Noack, 2000; Skjemstad et al., 2002). Unlike GAC, charcoal particles have underdeveloped pore structures and show porosity mainly in the ultramicropore region (3.5–7 Å) (Xiao and Pignatello, 2016). Natural charcoals are widespread in soils as a result of historical wildfires (III, 2020), land clearing, and crop residual burning (Lehmann and Joseph, 2009; Schmidt and Noack, 2000; Skjemstad et al., 2002), contributing to 30–50% of soil organic carbon in certain areas such as Midwest prairie soils (Glaser et al., 2001; Mao et al., 2012). Natural charcoals are similar in many respects to an engineered PCM form, commonly known as 'biochar' that has been modified such as to enhance its performance as an adsorbent in water and wastewater treatment. The polyaromatic surface of both GAC and biochar has been suggested to act as an electron shuttle, accelerating the redox conversion of organic compounds (Kappler et al., 2014; Millerick et al., 2013; Tang et al., 2011). Another question arises whether charcoals/biochars can alter the thermal degradation of PFAS, which has critical implications not only for fate/transport studies of PFAS under natural thermal conditions (e.g., wildfires) but for designing effective carbonaceous adsorbents for PFAS.

This study was conducted to address the above questions and to better understand the thermal decomposition kinetics, products, and pathways of PFAS, focusing on the effect of GAC and charcoals/biochars.

2. Materials and methods

2.1. PFAS chemicals

The test chemical set for thermal treatments included PFOS and five PFCAs — perfluorobutyric acid (PFBA), PFOA, perfluorononanoic acid (PFNA), perfluorodecanoic acid (PFDA), and perfluoroundecanoic acid (PFUnDA) (Supplementary data, Table S1). The test set also included one perfluoroalkyl ether carboxylic acid (PFECA) — hexafluoropropylene oxide dimer acid (HFPO-DA). The ammonium salt of HFPO-DA (trade name, GenX) is a new alternative to PFOA/PFOS that has been detected in surface and drinking water (Heydebreck et al., 2015; Strynar et al., 2015; Xiao, 2017). To confirm decomposition products, reference standards of perfluoropentanoic acid (PFPeA) and PFHpA were also prepared.

2.2. Thermal treatments (T#1)

The thermal decomposition of the studied PFAS was performed in a closed borosilicate glass container (Xiao et al., 2020) (see the Supplementary document) in three conditions (T#1, T#2, T#3), as shown in Fig. 1. Before the thermal treatment in T#1 (thermolysis), a known quantity (1.2×10^{-5} mol or 0.005 g PFOA) of PFAS chemical powders or solution (in the case of PFBA and HFPO-DA) was added into a pre-cleaned container and air-dried at 25 °C. The measurement of the weight or volume of PFAS chemicals became less accurate below 1.2×10^{-5} mol of PFAS. The container with PFAS was then capped with a ground glass stopper. Next, we set a muffle furnace (Neytech., Vulcan 3–550, USA) to a predetermined temperature (150 °C, 200 °C, 250 °C, 300 °C, or 400 °C), and then put the container with PFAS inside the furnace for an isothermal treatment for up to 180 min. After heat treatment and cooldown, the container was added with distilled water (DW) or methanol (amended with 100 mmol/L ammonium acetate) (Xiao et al., 2020) and sonicated for 30 min. Concentrations of fluoride ions (F^-) in DW and residual PFAS in methanol were determined (see the Supplementary document) (Xiao et al., 2020), and their masses (M_F and $M_{PFAS,T}$, mol) were calculated in the manner described previously (Xiao et al., 2020). Our extraction method (methanol with ammonium acetate) achieved recoveries ranging from 80.4% to 111.8% for most of the PFAS compounds involved in this study (Xiao et al., 2020). Concentrations of F^- were determined by the standard SPADNS method (Rice et al., 2012). The analysis of PFAS was carried out on a Waters Acquity ultrahigh pressure liquid chromatography (UPLC) system coupled with a Waters high-definition quantitative time-of-flight mass spectrometer (ToF-MS) (Xiao et al.,

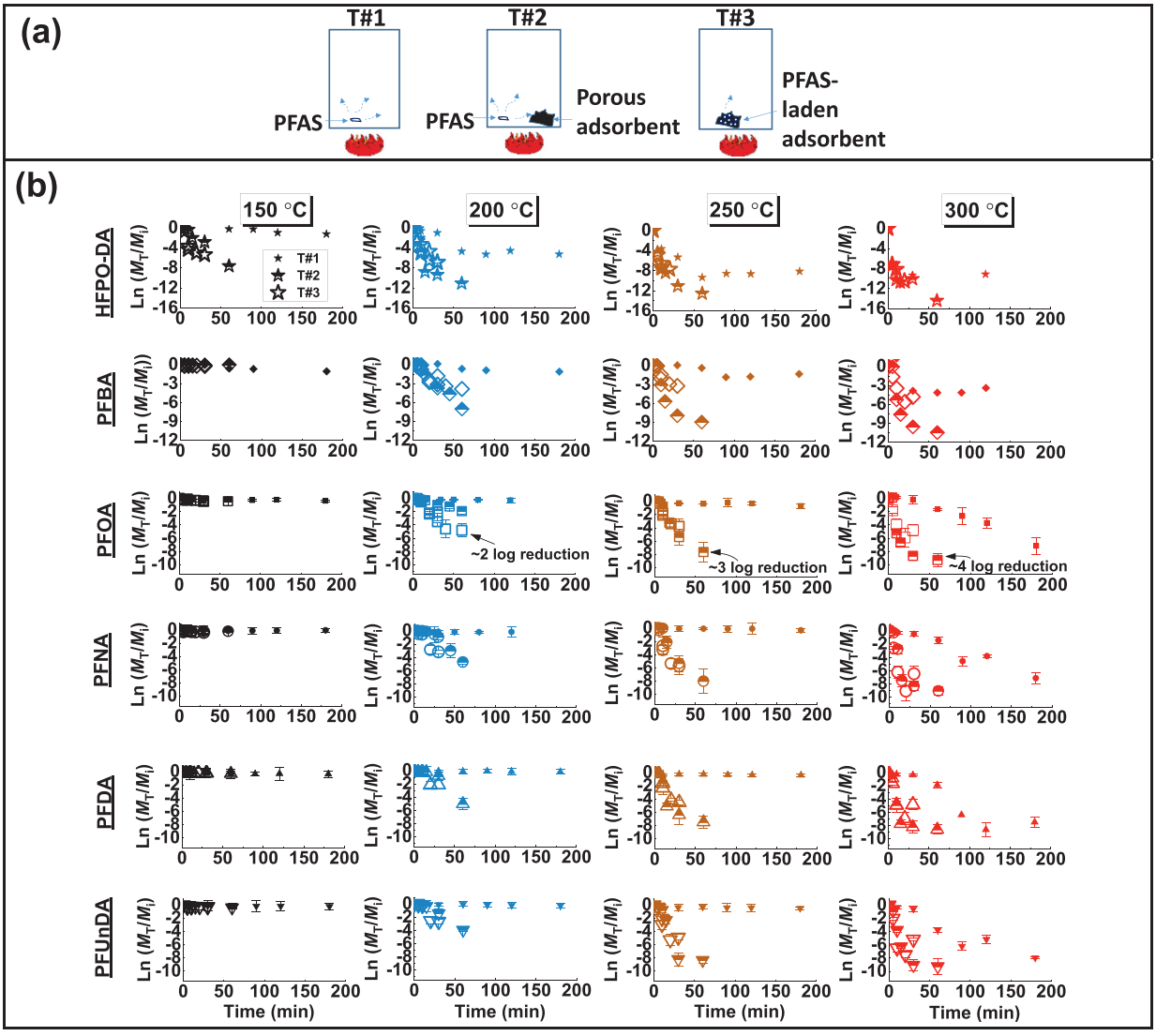

Fig. 1. (a) A schematic of PFAS thermal decomposition experiments in a closed system in three conditions (T#1, T#2, T#3). (b) Degradation of studied PFAS and a PFAS alternative (HFPO-DA) at various temperatures. Thermal treatments were triplicated for PFOA, PFNA, PFDA, and PFUnDA. The error bars represent the standard deviation (1-sigma) of three trials. Some points without visible error bars have errors that are smaller than the symbol. T#1 (closed symbols): PFAS only (initial PFAS mass: 1.2×10^{-5} mol). T#2 (half-open symbols): PFAS (1.2×10^{-5} mol) with the presence of 0.1 g GAC. T#3 (open symbols): 0.1 g of GAC laden with 3.0–4.5 $\times 10^{-7}$ mol PFAS. M_T and M_i are the residual mass of PFAS in heated samples and the initial mass in non-heated controls, respectively. The degradation of studied PFAS at 150 °C occurred at a slow rate (see Fig. 2 for decomposition rate constants).

2018) (Synapt G2-S, Waters Corporation, Milford, MA, USA) available in the Department of Biomedical Sciences of University of North Dakota. Figs. S1–S14 show representative chromatographic and spectral data.

The thermal decomposition efficiency was calculated by comparing the residual mass of PFAS in heated samples ($M_{PFAS,T}$, mol) with that in the non-heated controls ($M_{PFAS,i}$, mol).

The yield of F from a PFAS with $(2n + 1)$ F atoms during thermal decomposition was calculated with the following equation:

$$\text{Yield (F)} = \frac{M_F}{(2n+1)[M_{PFAS,i} - M_{PFAS,T}]} \times 100\% \quad (1)$$

The yield of transient intermediates from a parent compound was calculated by

$$\text{Yield (intermediate)} = \frac{M_{intermediate,formed}}{[M_{PFAS,i} - M_{PFAS,T}]} \times 100\% \quad (2)$$

2.3. Thermal treatments (T#2)

The thermal treatment in T#2 was performed similarly to that in T#1, except for the addition of a small amount of a porous adsorbent (Fig. 1). The mixture in the container was shaken manually for homogenization before thermal treatment. These porous adsorbents included GAC (Filtrasorb 200, Calgon Carbon Corporation, PA), raw charcoals ($n = 4$), and thermally air oxidized charcoals ($n = 4$). Two charcoal samples were made from a cellulose-rich feedstock (Maple wood) at a heat treatment temperature of 350 °C (referred as M350) or 600 °C (M600) following a previously published procedure (Xiao and Pignatello, 2015a, b). Another two charcoal samples were produced from a lignin-rich feedstock (pecan shells) at a heat treatment temperature of 350 °C (P350) or 700 °C (P700). We also prepared porosity-enhanced charcoals by oxidizing raw charcoals in air at 400 °C for 30 min (Cao et al., 2019; Xiao and Pignatello, 2016). The surface areas (SAs) of these PCMs were measured with N_2 at 77 K (Autosorb-iQ, Quantachrome, Boynton Beach, FL) (Xiao et al., 2019), and calculated by the 11-

point Brunauer–Emmett–Teller (BET) method. In addition to these carbonaceous materials, we also included a crosslinked polystyrene copolymer resin (Amberlite® XAD-2, Sigma–Aldrich, St. Louis, MO) as an adsorbent in a T#2 experiment. Finally, to examine the possible effect of borosilicate glass, a sample of PFOA was thermally treated along with five 2-mL borosilicate vials (available SA: 0.0027 m^2 per vial) to increase the available SA of the borosilicate glass container (0.025 m^2) by ~50%.

2.4. Thermal treatments (T#3)

To prepare the thermal treatment in T#3, a PFAS chemical was pre-adsorbed to a porous adsorbent in water. We could not conduct gas-phase adsorption experiments because the thermal decomposition of PFCA vapor is inevitable with increasing temperature to or above 150 °C. The test solution was prepared with distilled water containing 1.0×10^{-3} mol/L $NaHCO_3$ as a buffer and 1.0×10^{-3} mol/L NaCl. The adsorption experiment was performed in 50-mL Thermo Scientific Nunc™ sterile polypropylene vials rotated end-over-end at 10 rpm for four days at ~22 °C. An apparent adsorption equilibrium was reached within four days.

After adsorption, PFAS-laden adsorbent particles were split into two portions. The first portion was freeze-dried, weighed, and extracted using methanol (V_{extr}, mL) amended with 100 mmol/L ammonium acetate (NH_4Ac) (Xiao et al., 2020) to determine the mass before thermal treatment ($M_{PFAS,i}$). The one-point water–adsorbent distribution coefficient is defined as the ratio of the adsorbed concentration (C_s) to the dissolved concentration at equilibrium (C_w), $K_{d,w-s} = C_s/C_w$. The second portion of the PFAS-laden adsorbent particles was placed in a closed container and heated in an air environment within a muffle furnace (Neytech., Vulcan 3-550, USA) at a predetermined temperature. After heat treatment and cooldown, the sample was processed in the same way as described above for the T#1 experiment.

2.5. Other thermal treatments

We also performed thermal decomposition in the atmosphere of N_2. In this experiment, the sample to be heated was first placed into a container, and purged with N_2 for 15 min to remove air. The container was then capped with a ground glass stopper and heated in the muffle furnace at a pre-determined temperature.

In addition to isothermal treatment, we also examined the decomposition of PFAS in a dynamic thermal environment. Briefly, a known quantity of PFOA/PFOS chemical powders was placed in a closed container and heated dynamically in the muffle furnace at a 10 °C/min heating rate. This heating rate was used previously in the thermogravimetric analysis (TGA) (Xiao et al., 2020). After heat treatment and cooldown, the samples were treated in the same manner as the T#1 experiment.

Finally, the thermal decomposition of PFOA (Xiao et al., 2020) and PFOS at low and moderate temperatures (≤500 °C) was investigated by means of a thermal desorption–pyrolysis system (CDS Analytical) connected to a gas chromatograph with an MS detector (TD–Pyr–GC–MS) (Agilent GC 7890 and 5975C MS; Santa Clara, CA) (see the Supplementary data for more details).

3. Results and discussion

3.1. Thermal decomposition of PFAS in three conditions

We found that the thermal decomposition of PFAS mostly followed first-order kinetics at temperatures of 150–250 °C, in which the residual PFAS mass ($M_{PFAS,T}$) decreased in an exponential manner over heating time (Fig. 1). At a higher temperature (300 °C), the decomposition of these chemicals can also be described by second-order kinetics, in which a plot of $1/M_{PFAS,T}$ versus heating time is approximately linear. For comparison purposes, we used the first-order decomposition rate constant (k_{1st}, min^{-1}) in the following discussion.

The value of k_{1st} was below 0.005 min^{-1} for PFCAs at 150–250 °C in T#1 (Fig. 2). PFECA (HFPO-DA) appears to be more easily degraded than the PFCA with the same number of perfluorinated carbons (i.e., PFBA) (Figs. 1 and 2). This is consistent with our previous observation (Xiao et al., 2020) that the perfluorinated chain becomes less thermally stable with the inclusion of a foreign group (i.e., the ether group in HFPO-DA).

3.2. Effect of GAC

As illustrated in Fig. 2, GAC accelerated the thermal decomposition of HFPO-DA at temperatures as low as 150 °C in T#2 and T#3 conditions. The GAC-induced acceleration was evident for PFCAs at 200 °C, and up to a 60-fold increase in k_{1st} was observed (T#2 and T#3) (Fig. 2). This acceleration became even more significant at 250 °C, which led to a 150-fold increase in k_{1st} for PFUnDA (Fig. 2). As displayed in Fig. 2, the acceleration effect was less pronounced for the short-chain PFAS (PFBA) because the adsorption of PFBA on GAC was much weaker than that of its long-chain homologues (see Fig. S15 for adsorption isotherms of PFBA, HFPO-DA, and PFOA on GAC in the Supplementary document). The effect of GAC became less marked at higher temperatures of 300 °C and 400 °C at which the significant thermolysis (T#1) of PFCAs was seen (Figs. 1 and 2). A thermal treatment at 300 °C in T#2 led to near complete decomposition (>99.99%) of PFOA within 60 min. No attempt was made to maximize the thermal decomposition of PFCAs. A similar effect of GAC was observed when the samples were heated anaerobically (Fig. S16 of the Supplementary data); the k_{1st} of PFOA obtained in air was not significantly different from that obtained in N_2 (Fig. S16).

Because PFCEA and PFCA molecules were not pre-adsorbed on GAC in T#2 treatments, we hypothesize that the accelerated decomposition was caused by the adsorption of gas-phase PFCEA/PFCA on GAC that is much more thermally conductive (0.4–1.36 W/(m•K)) than air (<0.032 W/(m•K) at ≤100 °C) (Jin et al., 2013; Khaliji Oskouei and Tamainot-Telto, 2019). The heat transfer is more efficient on GAC than in air. On the other hand, the thermal conductivity of air increases with temperature. At 400 °C, the effect of GAC amendment on the thermal decomposition rate of PFAS appears to be much less important.

3.3. Effect of other PCMs and porous resin

To test this hypothesis, we conducted T#2 experiments with various PCMs and one non-carbonaceous material, XAD-2 resin. The results are plotted as a function of the $K_{d,w-s}$ of PFOA (Fig. 3). Charcoals have a higher thermal conductivity, 0.08–0.18 W/(m•K) (Behazin et al., 2016), than air. However, raw charcoals are primarily microporous (≤20 Å) (Xiao and Pignatello, 2016). Steric hindrance can result from narrow pore throats, internal obstructions, or pore blockage by occluded non-covalently bound matter such as pyrolysis tars (Xiao and Pignatello, 2015a; Zhu et al., 2005). The length of PFOA molecules is approximately 10 Å (Xiao et al., 2011). The steric bulk of PFOA molecules may limit their access to the interior micropore SA of raw charcoal that is available to N_2 molecules. Therefore, a low adsorption of PFOA on raw charcoals was observed (Fig. 3), and the thermal decomposition of PFOA was not accelerated with the addition of a raw charcoal sample (M350, M600, P350, or P700). The thermal air oxidation of raw charcoals caused pore wall etching and/or unclogging of pores bearing tarry deposits generated during the carbonization step (Xiao et al., 2017; Xiao and Pignatello, 2016). This in turn widened pores of charcoal

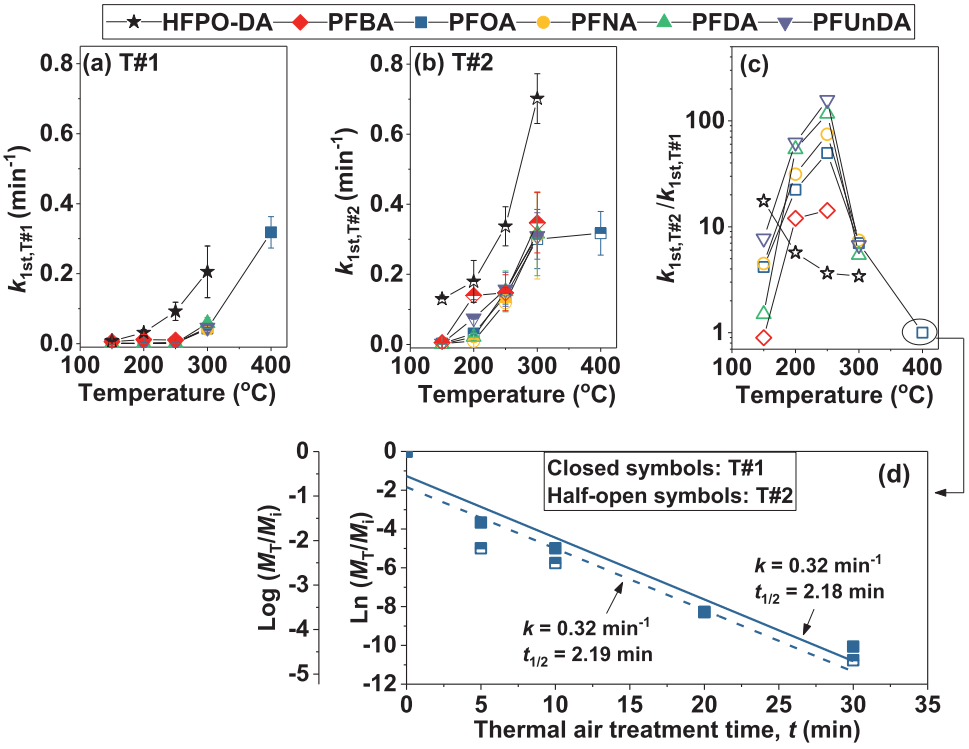

Fig. 2. (a–c) First-order decomposition rate constants (k_{1st}, min^{-1}) of PFCAs (1.2×10^{-5} mol) treated at different temperatures in conditions of T#1 (thermolysis; closed symbols) and T#2 (with the presence of 0.1 g of GAC; half-open symbols). (d) Thermal decomposition of PFOA (1.2×10^{-5} mol) in T#1 and T#2 (with the presence of 0.1 g GAC) in a closed container at 400 °C. Lines in (d) represent the best-fit to the decomposition data using the first-order kinetic model.

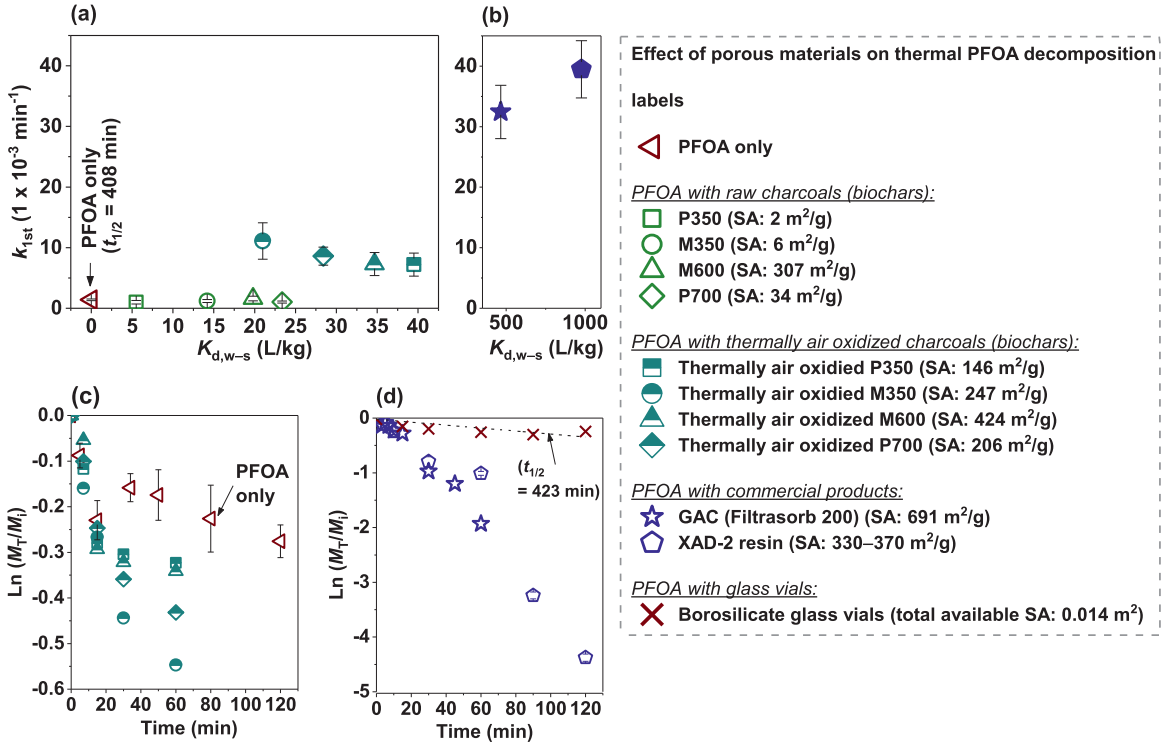

Fig. 3. (a) and (b): First-order decomposition rate constants (k_{1st}, 1×10^{-3} min^{-1}) of PFOA (1.2×10^{-5} mol) treated at 200 °C in T#1 (thermolysis) or in T#2 with the presence of a raw charcoal sample (M350, M600, P350, or P700) (0.5 g), a thermally air oxidized charcoal (0.1 g), GAC (Filtrasorb 200) (0.1 g), a non-carbonaceous porous material (XAD-2 resin) (0.1 g), or five 2-mL borosilicate vials (11.1 ± 0.01 g). (c) and (d): Thermal decomposition of PFOA in different conditions at 200 °C. The dashed line in (d) represents the best-fit to the decomposition data using the first-order kinetic model. The N_2 B.E.T. SA of XAD-2 resin was obtained from the literature (Jung et al., 2001; Tewari and Singh, 2002). The N_2 B.E.T. SAs of nine PCM adsorbents were measured in this study.

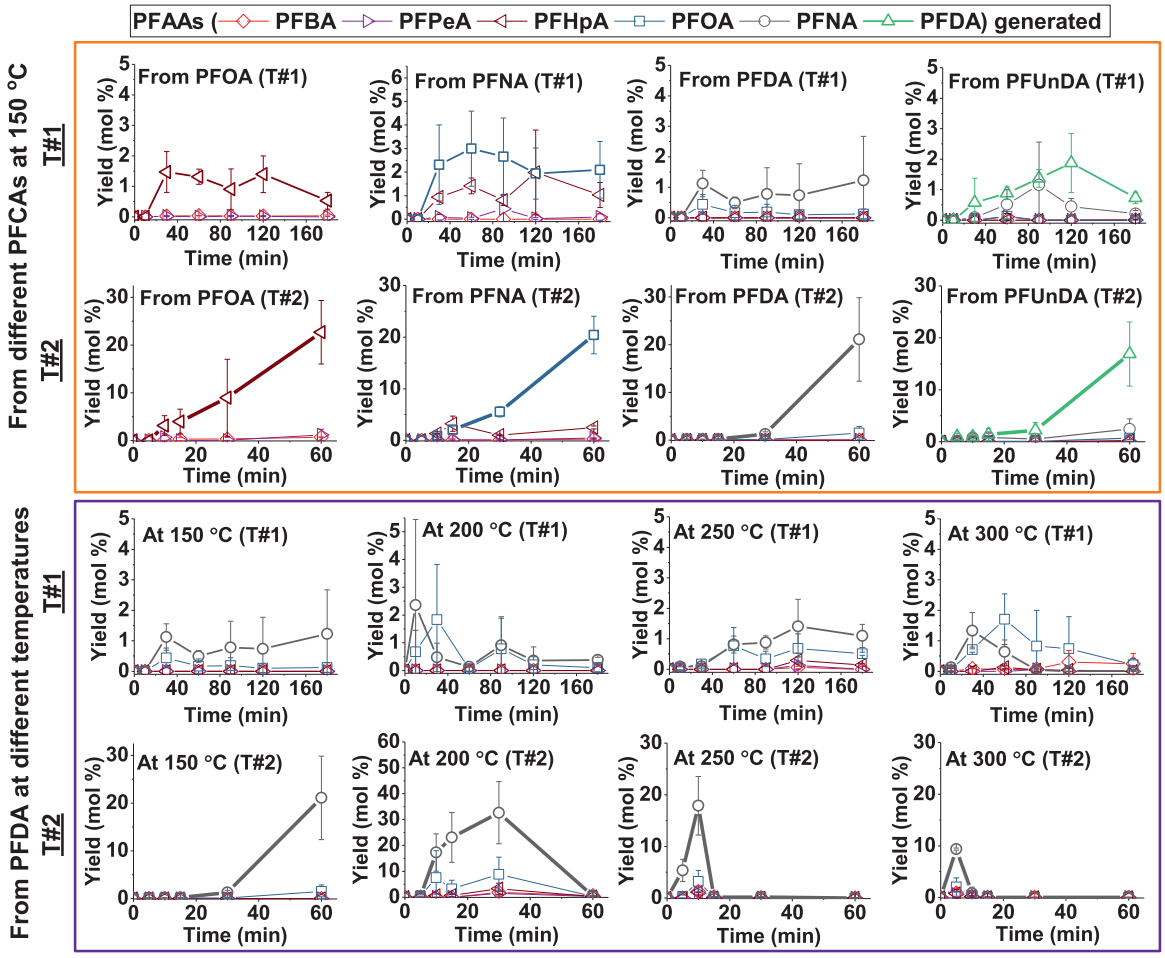

Fig. 4. Generation (and subsequent decomposition) of intermediate short-chain PFCAs from parent compounds treated in different conditions (T#1 and T#2; Fig. 1). The intermediates were detected by the UPLC–QToF-MS/MS method as detailed in the Supplementary data. Note the difference in y-axis scales.

and created new SA, which helped relieve steric hindrance for adsorption of PFOA molecules (Fig. 3). As illustrated in Fig. 3, the thermal decomposition of PFOA increased significantly with the addition of a thermally air oxidized charcoal. Commercial porous materials, GAC (or activated charcoal) and XAD-2 resin, adsorbed PFOA strongly (Fig. 3), reducing the thermal decomposition half-life of PFOA from ~400 min to less than 25 min at 200 °C (Fig. 3). The N_2 B.E.T. SA of the XAD-2 resin (330–370 m^2/g) is lower than that of the thermally air oxidized M600; however, the XAD-2 resin is characterized by a broad pore size distribution and a mean pore size of 90 Å. Mesopores (20–500 Å) have shown to be important for molecules to access deeper and smaller pores of adsorbents (Xiao and Pignatello, 2015a). Finally, the borosilicate glass appeared to have no significant effect on the thermal decomposition of PFOA (Fig. 3).

3.4. Thermal decomposition pathways

PFCAs yielded several transient intermediates at temperatures as low as 150 °C (Figs. 4 and S2). For a parent PFCA with *n* perfluorinated carbons, the highest yielding intermediate product is usually the shorter-chained PFCA with (*n* – 1) perfluorinated carbons (Figs. 4 and S2). For example, PFDA yielded shorter-chain PFCAs in the following order, PFNA > PFOA > PFHpA ≈ PFPeA ≈ PFBA. Similarly, the highest yielding byproduct of PFOA was PFHpA, whereas PFBA was a trace intermediate product. This formation pattern seems to agree with the stepwise defluorination mechanism (Pathway II in Fig. 5) that has been developed for photocatalysis (Wang et al., 2008), reduction by hydrated electrons (Bentel et al., 2019), and plasma (Singh et al., 2019) treatments of PFAS compounds. However, a closer look at the results reveals that it is not the predominant mechanism of the thermolysis of PFAS. First, the yield of intermediate PFCAs is low (<5 mol%) during the T#1 treatment (Fig. 4). Second, a clear stepwise pattern was not observed because all the short-chain intermediates appeared nearly simultaneously (Figs. 4 and S2).

We propose a different thermal decomposition mechanism (Pathway I in Fig. 5). We believe thermal decomposition of PFAS involves multistep radical chain reactions, including initiation, chain propagation, recombination, and termination (Xiao et al., 2021). Because of the strong C–F bond, we believe that the thermal decomposition of PFOA was initiated with the (homolytic) cleavage of the relatively weak C–C bond located next to the carboxyl group of PFOA or the C–S bond next to the sulfonate group of PFOS. The C–C or C–S bond splits, forming a nonfluorinated moiety and a perfluoroalkyl biradical such as :C_7F_{14} (*m/z* 350.0) from PFOA or :C_8F_{16} (*m/z* 399.9) from PFOS (Figs. 6 and S4). The perfluoroalkyl radical further undergoes a series of defluorination, or radical chain propagation reactions, generating shorter-chained perfluoroalkyl radicals (Fig. 5). These perfluoroalkyl radicals may recombine with carboxyl group/radical successively yielding PFCA intermediates. Eventually, these chain propagation reactions are terminated by producing the "dead," or very short, fluorinated units. In Pathway I, transient PFCA intermediates are the minor product. A number of interme-

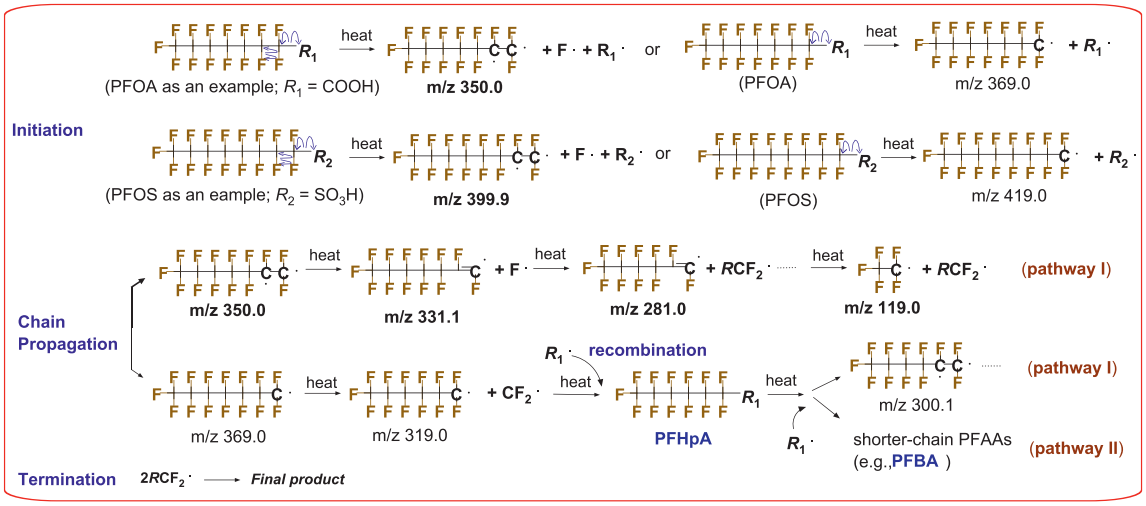

Fig. 5. Possible "unzip" decomposition pathways of perfluoroalkyl substances during thermal treatment. Species with *m/z* 399.9, 350.0, 331.1, 281.0, and 119.0 were shown in TD–Pyr–GC–MS spectra of PFOA (Xiao et al., 2020) and PFOS (Fig. S17). We found no MS spectral evidence for :C_7F_{14} (*m/z* 300.1), •C_6F_{13} (*m/z* 319.0), •C_7F_{15} (*m/z* 369.0), and •C_8F_{17} (*m/z* 419.0), but this does not preclude their formation in small amounts.

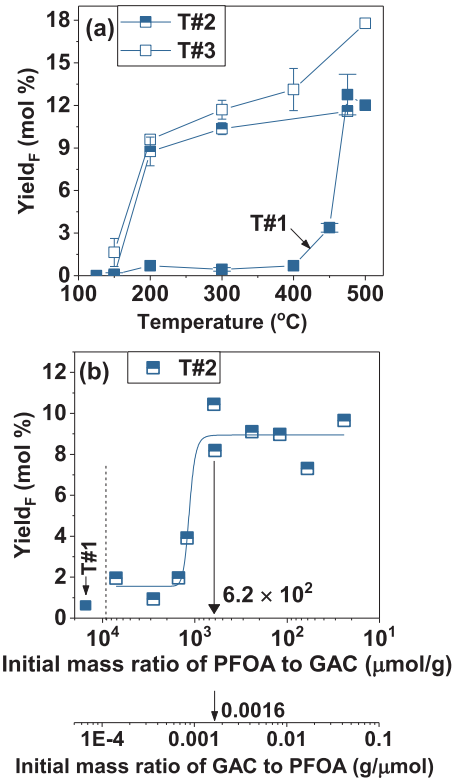

Fig. 6. (a) Measured yield of F from PFOA heated at different temperatures in three conditions, T#1 (1.2×10^{-5} mol PFOA), T#2 (1.2×10^{-5} mol PFOA with 0.1 g GAC), and T#3 (0.1 g of GAC laden with 3.1×10^{-7} mol PFOA). (b) Measured yield of F from PFOA heated in T#2 at 200 °C at different initial mass ratios of PFOA to GAC. All the data were obtained after 30-min isothermal heating of PFOA or PFOA with GAC. No measurable F was detected from GAC itself in thermal treatments.

diate perfluoroalkyl radicals/species were identified (Fig. S17), including ·CF_3 (*m/z* 69.0), •C_3F_3 (*m/z* 93.0), C_2F_4 (*m/z* 100.0), •C_2F_5 (*m/z* 119.0), •C_3F_5 (*m/z* 131.0), •C_3F_7 (*m/z* 169.0), •C_4F_7 (*m/z* 181.0), •C_5F_9 (*m/z* 231.0), •C_6F_{11} (*m/z* 281.0), •C_7F_{13} (*m/z* 331.0), and :C_7F_{14} (*m/z* 350.0). Many of these perfluoroalkyl radicals have also been observed in previous studies on the thermal treatment of PFOS (Wang et al., 2013) and perfluorocarbons (Kagramanov et al., 1990). Note that these species were detected by TD–Pyr–GC–MS in an inert atmosphere (helium). At present, our TD–Pyr–GC–MS system is not able to operate in an air atmosphere. However, the general decomposition mechanism (initiation, chain propagation, termination) illustrated in Fig. 5 may also apply to the thermal treatment of PFAS under active atmospheres.

It is evident that the presence of GAC altered the decomposition pathway of PFCAs, significantly increasing yields of shorter-chained PFCA intermediates at 150 °C (Figs. 4 and S3). At 200 °C, the yield of PFNA from PFDA was maximized after a 30-min treatment in T#2, and then disappeared on the same time scale as the parent compound (i.e., PFDA) (Figs. 4 and S3). At a higher temperature (300 °C), the yield of PFNA from PFDA dropped to <10 mol% after 5 min (Figs. 4 and S3), and was negligibly low with a longer heating time as PFNA quickly decomposed (Fig. 1). Previously, no measurable shorter-chained PFCAs were detected after a 30-min thermal treatment of PFOA on GAC at 400 °C (Xiao et al., 2020).

3.5. Effect of GAC on the yield of F from PFOA

The yield of F from PFOA during low-temperature T#1 thermolysis (≤400 °C) remained less than 2 mol% (Fig. 6). The addition of GAC (T#2) significantly enhanced the yield of F (Fig. 6a). We observed a critical mass ratio of PFOA to GAC (620 μmol PFOA/g_{GAC}) above which the effect of GAC is insignificant in T#2 as the GAC may become saturated with gas-phase PFOA molecules (Fig. 6b). This ratio reflects a dynamic balance between the adsorption and thermal decomposition of gas-state PFOA on the surface of GAC; it is more than one order of magnitude greater than the saturated adsorption amount (~40 μmol PFOA/g_{GAC}), or the maximum adsorption capacity, of the GAC for PFOA in the liquid phase (Fig. S15).

3.6. Three temperature zones

According to dynamic decomposition results (Fig. 7), three temperature zones can be recognized. PFOA is stable and essentially nonvolatile at temperatures below 90 °C (Zone A). A rise in temperature above 90 °C (Zone B) triggers the phase transfer (e.g., melting, boiling, sublimation) of PFOA molecules (Xiao et al., 2021) because of the rising vapor pressure (Kaiser et al., 2005). PFOA molecules started to degrade in Zone B. When the temperature increased to 400 °C or above (Zone C), PFOA molecules were quickly

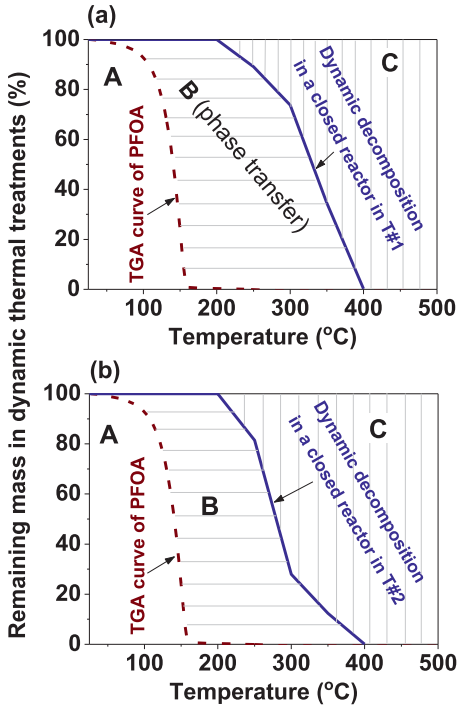

Fig. 7. Brown dashed lines: dynamic (10 °C/min) TGA curves of PFOA determined in an open system (Xiao et al., 2020). Blue solid curves: mass loss of PFOA in dynamic (10 °C/min) thermal treatments performed in a closed container in two conditions: (a), T#1 (1.2×10^{-5} mol PFOA); (b), T#2 (1.2×10^{-5} mol PFOA with 0.1 g GAC).

degraded (Figs. 2d and 7). The addition of GAC compressed Zone B and facilitated the thermal decomposition of PFOA. PFOS, on the other hand, is highly nonvolatile until 400 °C (Xiao et al., 2020). The thermal decomposition of PFOS was not significantly affected with the presence of GAC (Fig. S18).

4. Conclusions

The fate of PFAS in thermal processes is poorly understood. PFCAs used as surface-active agents in non-stick cookware and fire-fighting foams are generally assumed to be thermally stable at low temperatures (<300 °C). Contradictory to this prevailing view, this study shows that the thermolysis of PFCAs occurs at low temperatures of 150–200 °C (Figs. 2 and 4), albeit slowly. We further demonstrated that the low-temperature (150–300 °C) thermal decomposition of PFCAs was accelerated by highly porous adsorbents. The effect of GAC is much less significant at ≥400 °C at which the thermolysis of PFOA was markedly faster. The results also indicate that: (1) the N_2-B.E.T. SA of adsorbents is a poor predictor of the adsorption of PFOA molecules, and (2) the polyaromatic units of PCMs appear to be unimportant.

Supplementary data

Supplementary data associated with this article can be found online, including UPLC–QToF-MS/MS methods, TD–Pyr–GC–MS method, representative chromatographic and spectral data (Figs. S1–S14), adsorption isotherms of selected PFAS on GAC (Fig. S15), thermal decomposition rate of PFOA in the atmosphere of N_2 (Fig. S16), TD–Pyr–GC–MS chromatograms and mass spectra of thermal decomposition products of PFOA and PFOS at different temperatures (Fig. 17), thermal decomposition of PFOS (Fig. S18).

Declaration of Competing Interest

The authors declare that they have no known competing financial interests or personal relationships that could have appeared to influence the work reported in this paper.

Acknowledgements

This work was supported by an Early Career Award from the U.S. Environmental Protection Agency Science to Achieve Results (STAR) Program (RD839660; FX), the Department of Defense Strategic Environmental Research and Development Program (ER21-185; FX), and the U.S. National Science Foundation CAREER Program (2047062; FX). PCS was also supported by a graduate fellowship supported by the US Geological Survey (FAR0025807). The UPLC and the hybrid QToF-MS/MS systems, available in the Department of Biomedical Sciences at the University of North Dakota, were purchased under the NIH funded COBRE Mass Spec Core Facility Grant 5P30GM103329–05 (M.Y.G.). YB was supported by the University of North Dakota Pilot Postdoctoral Program from the Office of Vice President for Research & Economic Development.

Supplementary materials

Supplementary material associated with this article can be found, in the online version, at doi:10.1016/j.watres.2021.117271.

References

Anumol, T., Dagnino, S., Vandervort, D.R., Snyder, S.A., 2016. Transformation of polyfluorinated compounds in natural waters by advanced oxidation processes. Chemosphere 144, 1780–1787. doi:10.1016/j.chemosphere.2015.10.070.

Appleman, T.D., Higgins, C.P., Quiñones, O., Vanderford, B.J., Kolstad, C., Zeigler-Holady, J.C., Dickenson, E.R., 2014. Treatment of poly- and perfluoroalkyl substances in U.S. full-scale water treatment systems. Water Res. 51, 246–255. doi:10.1016/j.watres.2013.10.067.

Barzen-Hanson, K.A., Roberts, S.C., Choyke, S., Oetjen, K., McAlees, A., Riddell, N., McCrindle, R., Ferguson, P.L., Higgins, C.P., Field, J.A., 2017. Discovery of 40 classes of per- and polyfluoroalkyl substances in historical aqueous film-forming foams (AFFFs) and AFFF-impacted groundwater. Environ. Sci. Technol. 51 (4), 2047–2057. doi:10.1021/acs.est.6b05843.

Begley, T., Castle, L., Feigenbaum, A., Franz, R., Hinrichs, K., Lickly, T., Mercea, P., Milana, M., O'Brien, A., Rebre, S., Rijk, R., Piringer, O., 2005. Evaluation of migration models that might be used in support of regulations for food-contact plastics. Food Addit. Contam. Part A 22 (1), 73–90. doi:10.1080/02652030400028035.

Behazin, E., Ogunsona, E., Rodriguez-Uribe, A., Mohanty, A.K., Misra, M., Anyia, A.O., 2016. Mechanical, chemical, and physical properties of wood and perennial grass biochars for possible composite application. BioResources 11 (1), 1334–1348.

Belkouteb, N., Franke, V., McCleaf, P., Kohler, S., Ahrens, L., 2020. Removal of per- and polyfluoroalkyl substances (PFASs) in a full-scale drinking water treatment plant: long-term performance of granular activated carbon (GAC) and influence of flow-rate. Water Res. 182. doi:10.1016/j.watres.2020.115913.

Bentel, M.J., Yu, Y.C., Xu, L.H., Li, Z., Wong, B.M., Men, Y.J., Liu, J.Y., 2019. Defluorination of per- and polyfluoroalkyl substances (PFASs) with hydrated electrons: structural dependence and implications to PFAS remediation and management. Environ. Sci. Technol. 53 (7), 3718–3728. doi:10.1021/acs.est.8b06648.

Boiteux, V., Dauchy, X., Rosin, C., Munoz, J.F., 2012. National screening study on 10 perfluorinated compounds in raw and treated tap water in France. Arch. Environ. Contam. Toxicol. 63 (1), 1–12. doi:10.1007/S00244-012-9754-7.

Cao, X.Y., Xiao, F., Duan, P., Pignatello, J.J., Mao, J.D., Schmidt-Rohr, K., 2019. Effects of post-pyrolysis air oxidation on the chemical composition of biomass chars investigated by solid-state nuclear magnetic resonance spectroscopy. Carbon 153, 173–178. doi:10.1016/j.carbon.2019.07.004.

Council, N.R., 2009. Disposal of Activated Carbon from Chemical Agent Disposal Facilities. National Academies Press, Washington, D.C 1 online resource (xvi, 70 pages.

DeWitt, J.C., Blossom, S.J., Schaider, L.A., 2018. Exposure to per-fluoroalkyl and polyfluoroalkyl substances leads to immunotoxicity: epidemiological and toxicological evidence. J. Expo. Sci. Environ. Epidemiol. doi:10.1038/s41370-018-0097-y.

Duchesne, A.L., Brown, J.K., Patch, D.J., Major, D., Weber, K.P., Gerhard, J.I., 2020. Remediation of PFAS-contaminated soil and granular activated carbon by smoldering combustion. Environ. Sci. Technol. doi:10.1021/acs.est.0c03058.

Ericson, I., Domingo, J.L., Nadal, M., Bigas, E., Llebaria, X., van Bavel, B., Lindstrom, G., 2009. Levels of perfluorinated chemicals in municipal drinking water from Catalonia, Spain: public health implications. Arch. Environ. Contam. Toxicol. 57 (4), 631–638. doi:10.1007/s00244-009-9375-y.

Eschauzier, C., Beerendonk, E., Scholte-Veenendaal, P., de Voogt, P., 2012. Impact of treatment processes on the removal of perfluoroalkyl acids from the drinking water production chain. Environ. Sci. Technol. 46 (3), 1708–1715. doi:10.1021/es201662b.

Glaser, B., Haumaier, L., Guggenberger, G., Zech, W., 2001. The 'Terra Preta' phenomenon: a model for sustainable agriculture in the humid tropics. Naturwissenschaften 88 (1), 37–41. doi:10.1007/S001140000193.

Glover, C.M., Quinones, O., Dickenson, E.R.V, 2018. Removal of perfluoroalkyl and polyfluoroalkyl substances in potable reuse systems. Water Res. 144, 454–461. doi:10.1016/j.watres.2018.07.018.

Grandjean, P., Andersen, E.W., Budtz-Jorgensen, E., Nielsen, F., Molbak, K., Weihe, P., Heilmann, C., 2012. Serum vaccine antibody concentrations in children exposed to perfluorinated compounds. JAMA 307 (4), 391–397.

Heydebreck, F., Tang, J., Xie, Z., Ebinghaus, R., 2015. Alternative and legacy perfluoroalkyl substances: differences between European and Chinese river/estuary systems. Environ. Sci. Technol. 49 (14), 8386–8395. doi:10.1021/acs.est.5b01648.

Hoffman, K., Webster, T.F., Bartell, S.M., Weisskopf, M.G., Fletcher, T., Vieira, V.M., 2011. Private drinking water wells as a source of exposure to perfluorooctanoic acid (PFOA) in communities surrounding a fluoropolymer production facility. Environ. Health Perspect. 119 (1), 92–97. doi:10.1289/ehp.1002503.

Houtz, E.F., Higgins, C.P., Field, J.A., Sedlak, D.L., 2013. Persistence of perfluoroalkyl acid precursors in AFFF-impacted groundwater and soil. Environ. Sci. Technol. 47 (15), 8187–8195. doi:10.1021/es4018877.

Houtz, E.F., Sutton, R., Park, J.S., Sedlak, M., 2016. Poly- and perfluoroalkyl substances in wastewater: significance of unknown precursors, manufacturing shifts, and likely AFFF impacts. Water Res. 95, 142–149. doi:10.1016/j.watres.2016.02.055.

Insurance Information Institute (III) (2020) Wildfire statistics. http://www.iii.org/fact-statistic/wildfires (accessed December 2020).

Jin, B., Mallula, S., Golovko, S.A., Golovko, M.Y., Xiao, F., 2020. In vivo generation of PFOA, PFOS, and other compounds from cationic and zwitterionic per- and polyfluoroalkyl substances in a terrestrial invertebrate (Lumbricus terrestris). Environ. Sci. Technol. 54 (12), 7378–7387. doi:10.1021/acs.est.0c01644.

Jin, Z.Q., Tian, B., Wang, L.W., Wang, R.Z., 2013. Comparison on thermal conductivity and permeability of granular and consolidated activated carbon for refrigeration. Chin. J. Chem. Eng. 21 (6), 676–682. doi:10.1016/S1004-9541(13)60525-X.

Jung, M.W., Ahn, K.H., Lee, Y., Kim, K.P., Paeng, I.R., Rhee, J.S., Park, J.T., Paeng, K.J., 2001. Evaluation on the adsorption capabilities of new chemically modified polymeric adsorbents with protoporphyrin IX. J. Chromatogr. A 917 (1–2), 87–93. doi:10.1016/S0021-9673(01)00673-2.

Kagramanov, N.D., Kutin, A.A., Mysov, E.I., Makarov, K.N., Gervits, L.L., 1990. Mass spectrometric study of the pyrolysis of perfluorinated compounds of composition C_6F_{12}-C_9F_{20}, containing perfluoroisopropyl groups. Bull. Acad. Sci. Ussr Div. Chem. Sci. 39 (5), 925–930. doi:10.1007/Bf00961684.

Kah, M., Sigmund, G., Xiao, F., Hofmann, T., 2017. Sorption of ionizable and ionic organic compounds to biochar, activated carbon and other carbonaceous materials. Water Res. submitted.

Kaiser, M.A., Larsen, B.S., Kao, C.P.C., Buck, R.C, 2005. Vapor pressures of perfluorooctanoic, -nonanoic, -decanoic, -undecanoic, and -dodecanoic acids. J. Chem. Eng. Data 50 (6), 1841–1843. doi:10.1021/je050070r.

Kappler, A., Wuestner, M.L., Ruecker, A., Harter, J., Halama, M., Behrens, S., 2014. Biochar as an electron shuttle between bacteria and Fe(III) minerals. Environ. Sci. Technol. Lett. 1 (8), 339–344. doi:10.1021/ez5002209.

Khaliji Oskouei, Z., Tamainot-Telto, Z., 2019. Investigation of the heat transfer properties of granular activated carbon with R723 for adsorption refrigeration and heat pump. Therm. Sci. Eng. Progress 12, 1–12. doi:10.1016/j.tsep.2019.05.003.

Langberg, H.A., Breedveld, G.D., Gronning, H.M., Kvennas, M., Jenssen, B.M., Hale, S.E., 2019. Bioaccumulation of fluorotelomer sulfonates and perfluoroalkyl acids in marine organisms living in aqueous film forming foam (AFFF) impacted waters. Environ. Sci. Technol. 53 (18), 10951–10960. doi:10.1021/acs.est.9b00927.

Lee, H., D'eon, J., Mabury, S.A., 2010. Biodegradation of polyfluoroalkyl phosphates as a source of perfluorinated acids to the environment. Environ. Sci. Technol. 44 (9), 3305–3310. doi:10.1021/Es9028183.

Lehmann, J., Joseph, S., 2009. Biochar For Environmental Management: Science and Technology. Earthscan Publications Ltd., London, UK.

Liu, F., Hua, L., Zhang, W., 2020. Influences of microwave irradiation on performances of membrane filtration and catalytic degradation of perfluorooctanoic acid (PFOA). Environ. Int. 143, 105969. doi:10.1016/j.envint.2020.105969.

Mao, J.D., Johnson, R.L., Lehmann, J., Olk, D.C., Neves, E.G., Thompson, M.L., Schmidt-Rohr, K., 2012. Abundant and stable char residues in soils: implications for soil fertility and carbon sequestration. Environ. Sci. Technol. 46 (17), 9571–9576. doi:10.1021/Es301107c.

Melzer, D., Rice, N., Depledge, M.H., Henley, W.E., Galloway, T.S., 2010. Association between serum perfluorooctanoic acid (PFOA) and thyroid disease in the US national health and nutrition examination survey. Environ. Health Perspect. 118 (5), 686–692. doi:10.1289/ehp.0901584.

Millerick, K., Drew, S.R., Finneran, K.T., 2013. Electron shuttle-mediated biotransformation of hexahydro-1,3,5-trinitro-1,3,5-triazine adsorbed to granular activated carbon. Environ. Sci. Technol. 47 (15), 8743–8750. doi:10.1021/es401641s.

Nabb, D.L., Szostek, B., Himmelstein, M.W., Mawn, M.P., Gargas, M.L., Sweeney, L.M., Stadler, J.C., Buck, R.C., Fasano, W.J., 2007. In vitro metabolism of 8-2 fluorotelomer alcohol: interspecies comparisons and metabolic pathway refinement. Toxicol. Sci. 100 (2), 333–344. doi:10.1093/toxsci/kfm230.

NHANES, 2014. Fourth National Report On Human Exposure to Environmental Chemicals (updated tables).

Post, G.B., Cohn, P.D., Cooper, K.R., 2012. Perfluorooctanoic acid (PFOA), an emerging drinking water contaminant: a critical review of recent literature. Environ. Res. 116, 93–117. doi:10.1016/J.Envres.2012.03.007.

Rahman, M.F., Peldszus, S., Anderson, W.B., 2014. Behaviour and fate of perfluoroalkyl and polyfluoroalkyl substances (PFASs) in drinking water treatment: a review. Water Res. 50, 318–340. doi:10.1016/j.watres.2013.10.045.

Rice, E.W., Baird, R.B., Eaton, A.D., Clesceri, L.S., 2012. Standard Methods for the Examination of Water and Wastewater. American Public Health Association, Washington, D.C.

Sajid, M., Ilyas, M., 2017. PTFE-coated non-stick cookware and toxicity concerns: a perspective. Environ. Sci. Pollut. Res. 24 (30), 23436–23440. doi:10.1007/s11356-017-0095-y.

Schaefer, L.A., Balan, S.A., Blum, A., Andrews, D.Q., Strynar, M.J., Dickinson, M.E., Lunderberg, D.M., Lang, J.R., Peaslee, G.F., 2017. Fluorinated compounds in U.S. fast food packaging. Environ. Sci. Technol. Lett. 4, 105–111. doi:10.1021/acs.estlett.6b00435.

Schmidt, M.W.I., Noack, A.G, 2000. Black carbon in soils and sediments: analysis, distribution, implications, and current challenges. Glob. Biogeochem. Cycles 14 (3), 777–793. doi:10.1029/1999gb001208.

Schröder, H.F., Meesters, R.J.W, 2005. Stability of fluorinated surfactants in advanced oxidation processes – a follow up of degradation products using flow injection-mass spectrometry, liquid chromatography-mass spectrometry and liquid chromatography-multiple stage mass spectrometry. J. Chromatogr. A 1082 (1), 110–119. doi:10.1016/J.Chroma.2005.02.070.

Sinclair, E., Kannan, K., 2006. Mass loading and fate of perfluoroalkyl surfactants in wastewater treatment plants. Environ. Sci. Technol. 40 (5), 1408–1414. doi:10.1021/es051798v.

Singh, R.K., Fernando, S., Baygi, S.F., Multari, N., Thagard, S.M., Holsen, T.M., 2019. Breakdown products from perfluorinated alkyl substances (PFAS) degradation in a plasma-based water treatment process. Environ. Sci. Technol. 53 (5), 2731–2738. doi:10.1021/acs.est.8b07031.

Skjemstad, J.O., Reicosky, D.C., Wilts, A.R., McGowan, J.A., 2002. Charcoal carbon in U.S. agricultural soils. Soil Sci. Soc. Am. J. 66 (4), 1249–1255. doi:10.2136/sssaj2002.1249.

Steenland, K., Tinker, S., Shankar, A., Ducatman, A., 2010. Association of perfluorooctanoic acid (PFOA) and perfluorooctane sulfonate (PFOS) with uric acid among adults with elevated community exposure to PFOA. Environ. Health Perspect. 118 (2), 229–233. doi:10.1289/ehp.0900940.

Strynar, M., Dagnino, S., McMahen, R., Liang, S., Lindstrom, A., Andersen, E., McMillan, L., Thurman, M., Ferrer, I., Ball, C., 2015. Identification of novel perfluoroalkyl ether carboxylic acids (PFECAs) and sulfonic acids (PFESAs) in natural waters using accurate mass time-of-flight mass spectrometry (TOFMS). Environ. Sci. Technol. 49, 11622–11630. doi:10.1021/acs.est.5b01215.

Tang, H., Zhu, D., Li, T., Kong, H., Chen, W., 2011. Reductive dechlorination of activated carbon-adsorbed trichloroethylene by zero-valent iron: carbon as electron shuttle. J. Environ. Qual. 40 (6), 1878–1885. doi:10.2134/jeq2011.0185.

Tewari, P.K., Singh, A.K., 2002. Preconcentration of lead with Amberlite XAD-2 and Amberlite XAD-7 based chelating resins for its determination by flame atomic absorption spectrometry. Talanta 56 (4), 735–744. doi:10.1016/S0039-9140(01)00606-3.

Vestergren, R., Cousins, I.T., 2009. Tracking the pathways of human exposure to perfluorocarboxylates. Environ. Sci. Technol. 43 (15), 5565–5575.

Wang, F., Shih, K., Lu, X., Liu, C., 2013. Mineralization behavior of fluorine in perfluorooctanesulfonate (PFOS) during thermal treatment of lime-conditioned sludge. Environ. Sci. Technol. 47 (6), 2621–2627. doi:10.1021/es305352p.

Wang, Y., Zhang, P.Y., Pan, G., Chen, H., 2008. Ferric ion mediated photochemical decomposition of perfluorooctanoic acid (PFOA) by 254nm UV light. J. Hazard. Mater. 160 (1), 181–186. doi:10.1016/j.jhazmat.2008.02.105.

Watanabe, N., Takata, M., Takemine, S. and Yamamoto, K. (2018) Thermal mineralization behavior of PFOA, PFHxA, and PFOS during reactivation of granular activated carbon (GAC) in nitrogen atmosphere. Environ. Sci. Pollut. Res. Int.25(8), 7200–7205. doi:10.1007/s11356-015-5353-2

Xiao, F., 2017. Emerging poly- and perfluoroalkyl substances in the aquatic environment: a review of current literature. Water Res. 124, 482–495. doi:10.1016/j.watres.2017.07.024.

Xiao, F., Bedane, A.H., Zhao, J.X., Mann, M.D. and Pignatello, J.J. (2017) Thermal air oxidation changes surface and adsorptive properties of black carbon (char/biochar). The Science of the total environment 618, 276–283. doi:10.1016/j.scitotenv.2017.11.008

Xiao, F., Gulliver, J.S., Simcik, M.F., 2013a. Perfluorooctane sulfonate (PFOS) contamination of fish in urban lakes: a prioritization methodology for lake management. Water Res. 47 (20), 7264–7272. doi:10.1016/j.watres.2013.09.063.

Xiao, F., Halbach, T.R., Simcik, M.F., Gulliver, J.S., 2012. Input characterization of perfluoroalkyl substances in wastewater treatment plants: source discrimination by exploratory data analysis. Water Res. 46 (9), 3101–3109. doi:10.1016/j.watres.2012.03.027.

Xiao, F., Hanson, R.A., Golovko, S.A., Golovko, M.Y., Arnold, W.A., 2018. PFOA and PFOS are generated from zwitterionic and cationic precursor compounds during water disinfection with chlorine or ozone. Environ. Sci. Technol. Lett. 5 (6), 382–388. doi:10.1021/acs.estlett.8b00266.

Xiao, F., Jin, B., Golovko, S.A., Golovko, M.Y., Xing, B., 2019. Sorption and desorption mechanisms of cationic and zwitterionic per- and polyfluoroalkyl substances in natural soils: thermodynamics and hysteresis. Environ. Sci. Technol. 53 (20), 11818–11827. doi:10.1021/acs.est.9b05379.

Xiao, F., Pignatello, J.J., 2015a. Interactions of triazine herbicides with biochar: steric and electronic effects. Water Res. 80, 179–188. doi:10.1016/j.watres.2015.04.040.

Xiao, F., Pignatello, J.J., 2015b. π+–π interactions between (hetero)aromatic amine cations and the graphitic surfaces of pyrogenic carbonaceous materials. Environ. Sci. Technol. 49 (2), 906–914. doi:10.1021/es5043029.

Xiao, F., Pignatello, J.J., 2016. Effects of post-pyrolysis air oxidation of biomass chars on adsorption of neutral and ionizable compounds. Environ. Sci. Technol. 50 (12), 6276–6283. doi:10.1021/acs.est.6b00362.

Xiao, F., Sasi, P.C., Yao, B., Kubatova, A., Golovko, S.A., Golovko, M.Y., Soli, D, 2020. Thermal stability and decomposition of perfluoroalkyl substances on spent granular activated carbon. Environ. Sci. Technol. Lett. 7 (5), 343–350. doi:10.1021/acs.estlett.0c00114.

Xiao, F., Sasi, P.C., Yao, B., Kubatova, A., Golovko, S.A., Golovko, M.Y., Soli, D, 2021. Thermal Decomposition of PFAS: response to Comment on "Thermal Stability and Decomposition of Perfluoroalkyl Substances on Spent Granular Activated Carbon. in press. Environ. Sci. Technol. Lett. 8, 364–365.

Xiao, F., Simcik, M.F., Gulliver, J.S., 2013b. Mechanisms for removal of perfluorooctane sulfonate (PFOS) and perfluorooctanoate (PFOA) from drinking water by conventional and enhanced coagulation. Water Res. 47 (1), 49–56. doi:10.1016/j.watres.2012.09.024.

Xiao, F., Zhang, X., Penn, L., Gulliver, J.S., Simcik, M.F., 2011. Effects of monovalent cations on the competitive adsorption of perfluoroalkyl acids by kaolinite: experimental studies and modeling. Environ. Sci. Technol. 45 (23), 10028–10035. doi:10.1021/es202524y.

Yu, J., Hu, J.Y., Tanaka, S., Fujii, S., 2009a. Perfluorooctane sulfonate (PFOS) and perfluorooctanoic acid (PFOA) in sewage treatment plants. Water Res. 43 (9), 2399–2408. doi:10.1016/J.Watres.2009.03.009.

Yu, Q., Zhang, R., Deng, S., Huang, J., Yu, G., 2009b. Sorption of perfluorooctane sulfonate and perfluorooctanoate on activated carbons and resin: kinetic and isotherm study. Water Res. 43 (4), 1150–1158. doi:10.1016/j.watres.2008.12.001.

Zhu, D.Q., Kwon, S., Pignatello, J.J., 2005. Adsorption of single-ring organic compounds to wood charcoals prepared under different thermochemical conditions. Environ. Sci. Technol. 39 (11), 3990–3998. doi:10.1021/Es050129e.